

Article ID: 1001-3555(2016)02-0131-09

Catalytic Decomposition of N_2O over $Mn_xCo_{2.5-x}Al_{0.5}O_4$ Ternary Spinel Oxides

WU Cang-cang, ZHANG Hai-jie, WANG Jian, ZHENG Li, XU Xiu-feng*

(*Institute of Applied Catalysis, Yantai University, Yantai 264005, China*)

Abstract: A series of $Mn_xCo_{2.5-x}Al_{0.5}O_4$ ternary spinel oxides were prepared by sol-gel method for N_2O catalytic decomposition in the presence of oxygen. These catalysts were characterized by means of techniques such as nitrogen physisorption, X-ray diffraction(XRD), scanning electron microscopy(SEM), temperature-programmed reduction of hydrogen(H_2 -TPR), temperature-programmed desorption of oxygen(O_2 -TPD), and X-ray photoelectron spectroscopy(XPS). The effect of preparation parameters such as compositions, pH values of mother liquid, and potassium loadings on their catalytic activity has been investigated. The results show that K-modified catalysts exhibit better activity and higher resistance towards water due to the weakness of surface metal-oxygen bonds in contrast to un-modified catalyst, the $K/Mn_{0.2}Co_{2.3}Al_{0.5}O_4$ prepared using mother liquid of pH=2 and $K/(Mn+Co)$ molar ratio of 0.02 is the most active. In addition, 98.5% and 76.5% conversions of N_2O over $0.02K/Mn_{0.2}Co_{2.3}Al_{0.5}O_4$ could be maintained after continuous running for 50 h at 400 °C in atmosphere of oxygen and oxygen-steam together, respectively.

Key words: catalytic decomposition of N_2O ; ternary spinel oxides; $Mn_xCo_{2.5-x}Al_{0.5}O_4$; sol-gel method; K-modified catalysts
CLC number: O643.32 **Document code:** A

Anthropogenic N_2O emissions from some industrial processes such as the synthesis of adipic and nitric acids are increasing nowadays. N_2O is one of the most important green-house gases limited by Kyoto protocol, and has a high global warming potential (GWP) of 310 and long lifetime of 120 years^[1]. Furthermore, N_2O can destroy ozone in the atmosphere. Catalytic decomposition of N_2O to nitrogen and oxygen is considered as an effective and economic method. Several types of catalysts, such as supported noble metals^[2-4], ion-exchanged zeolites^[5-7], and transition metal oxides^[8-14], have been reported. Among these catalysts, cobalt-based mixed oxides with spinel structure are very attractive ones. It is reported that N_2O catalytic decomposition follows an oxidation-reduction(Redox) mechanism^[13-15], and appropriate loading of alkali or alkaline earth metal on catalysts surface can improve the catalytic activity^[16-23].

Recently, we prepared a series of Co-Al mixed oxides, such as $CoAl_2O_4$, $Co_{1.5}Al_{1.5}O_4$, Co_2AlO_4 , and $Co_{2.5}Al_{0.5}O_4$, by sol-gel method for N_2O decomposition, and found that the optimal catalyst was $Co_{2.5}Al_{0.5}O_4$ ^[24].

Based on the previous result, several ternary oxides of $Mn_xCo_{2.5-x}Al_{0.5}O_4$ were prepared and further modified by K_2CO_3 in this work. The effect of catalyst compositions, pH values of mother liquid, and potassium loadings on catalytic activity for N_2O decomposition in the presence of oxygen was investigated. In addition, the catalytic stability in atmosphere of oxygen-alone or oxygen-steam together was tested.

1 Experimental

1.1 Catalysts preparation

1.1.1 $Mn_xCo_{2.5-x}Al_{0.5}O_4$ catalysts with different compositions Aqueous solution containing stoichiomet-

Received date: 2016-01-30; **Revised date:** 2016-02-28.

Foundation: This work was financially supported by the Department of Science and Technology of Shandong Province (No. 2012GSF11708) and Graduate Innovation Foundation of Yantai University (GIFYTU).

First author: Wu Cang-cang (1990-), Female, Master candidate.

* **Corresponding author:** Tel: 0535-6902746, E-mail: xxf@ytu.edu.cn.

ric amounts of $\text{Co}(\text{NO}_3)_2$, $\text{Al}(\text{NO}_3)_3$ and $\text{Mn}(\text{NO}_3)_2$ with total cations concentration of $1 \text{ mol} \cdot \text{L}^{-1}$ was dropped into $1 \text{ mol} \cdot \text{L}^{-1}$ citric acid solution. The mixed solution with $\text{pH} = 2$ adjusted by 2.5% diluted ammonia was vigorously stirred at room temperature for 30 min. Then the solution was concentrated to a viscous state by using a rotary evaporator at $65 \text{ }^\circ\text{C}$, dried at $120 \text{ }^\circ\text{C}$ for 12 h to gain xerogel, and calcined at $600 \text{ }^\circ\text{C}$ for 4 h to get the Mn-Co-Al composite oxides. The catalysts were denoted as $\text{Mn}_x\text{Co}_{2.5-x}\text{Al}_{0.5}\text{O}_4$ ($x = 0, 0.2, 0.4, 0.6, 0.8, 1$).

1.1.2 $\text{Mn}_{0.2}\text{Co}_{2.3}\text{Al}_{0.5}\text{O}_4$ prepared by mother liquids with different pH values Mixed solution of $\text{Co}(\text{NO}_3)_2$, $\text{Al}(\text{NO}_3)_3$ and $\text{Mn}(\text{NO}_3)_2$ with total cations concentration of $1 \text{ mol} \cdot \text{L}^{-1}$ was dropped into $1 \text{ mol} \cdot \text{L}^{-1}$ citric acid solution, then 2.5% diluted ammonia was added drop-wise to the above mixed solution to adjust the pH values of mother liquid. After gelation, drying and calcinations, the catalysts were obtained and designated as $\text{Mn}_{0.2}\text{Co}_{2.3}\text{Al}_{0.5}\text{O}_4$ ($\text{pH} = y$), where y is the pH value of mother liquid.

1.1.3 K-modified $\text{Mn}_{0.2}\text{Co}_{2.3}\text{Al}_{0.5}\text{O}_4$ catalysts The $\text{Mn}_{0.2}\text{Co}_{2.3}\text{Al}_{0.5}\text{O}_4$ ($\text{pH} = 2$) was incipiently impregnated by K_2CO_3 solution with given concentration at room temperature for 24 h, dried at $120 \text{ }^\circ\text{C}$ for 12 h, and calcined at $600 \text{ }^\circ\text{C}$ for 4 h. The K-modified catalysts were denoted as $z\text{K}/\text{Mn}_{0.2}\text{Co}_{2.3}\text{Al}_{0.5}\text{O}_4$, where z stands for the molar ratio of $\text{K}/(\text{Mn}+\text{Co})$.

1.2 Catalytic decomposition of N_2O

N_2O decomposition was carried out in a fixed-bed reactor and 1 g catalyst ($0.900 \sim 0.280 \text{ mm}$) was used for each test. Unless otherwise stated, the reactant gases consisted of 2% N_2O , 4% O_2 and balanced argon with gas hourly space velocity (GHSV) of $8.4 \text{ L} \cdot \text{h}^{-1} \cdot \text{g}^{-1}$. For the catalytic test in oxygen-steam atmosphere, the feeds were 2% N_2O , 4% O_2 , 8.8% H_2O and balanced argon. The effluent stream was analyzed with gas chromatography (GC-920, Shanghai Haixin) equipped with a Porapak Q column and thermal conductivity detector (TCD).

N_2O conversion was calculated on the basis of N_2O concentration difference before and after reaction at each temperature for 30 min. To test the catalytic

stability, the reaction temperature was increased from room temperature to $400 \text{ }^\circ\text{C}$ at a ramp of $10 \text{ }^\circ\text{C} \cdot \text{min}^{-1}$, and kept at $400 \text{ }^\circ\text{C}$ for 50 h.

1.3 Catalysts characterization

X-ray diffraction (XRD) patterns were recorded on a powder X-ray diffractometer (XRD-6100, Shimadzu) with $\text{Cu K}\alpha$ radiation ($\lambda = 0.154 \text{ nm}$) and graphite monochromator at 40 kV and 30 mA. On the basis of diffraction data of crystallographic plane (311) attributed to spinel-structured materials, the crystallite size was calculated by Scherrer equation.

BET surface area was measured by low temperature nitrogen physisorption on a NOVA3000 apparatus (Quantachrome). Prior to the measurement, the catalyst sample was pre-treated at $300 \text{ }^\circ\text{C}$ for 2 h under vacuum to remove any impurities.

Temperature-programmed reduction of hydrogen (H_2 -TPR) was carried out on a chemical adsorption instrument (PCA-1200, Beijing Builder). Prior to the measurement, 80 mg catalyst was pre-treated in Ar flow ($20 \text{ mL} \cdot \text{min}^{-1}$) from room temperature to $500 \text{ }^\circ\text{C}$ and kept isothermally for 30 min. After cooling to room temperature, the catalyst was exposed to 10% H_2/Ar ($20 \text{ mL} \cdot \text{min}^{-1}$) and heated at a ramp of $10 \text{ }^\circ\text{C} \cdot \text{min}^{-1}$. The hydrogen consumption was recorded by TCD.

Temperature programmed desorption of oxygen (O_2 -TPD) was also performed using adsorption apparatus (PCA-1200, Beijing Builder). Before O_2 -TPD measurement, 100 mg catalyst was exposed to pure oxygen at $120 \text{ }^\circ\text{C}$ for 30 min. After cooling to ambient temperature and getting a smooth baseline, the catalyst was heated under pure helium at a ramping rate of $10 \text{ }^\circ\text{C} \cdot \text{min}^{-1}$, and the oxygen desorbed was measured by TCD.

The morphology of catalysts was observed with a scanning electron microscopy (SEM, S-4800, Hitachi). To improve the electric conductivity, the samples were coated previously with platinum by using an ion sputter (E-1045, Hitachi).

X-ray photoelectron spectra (XPS) of cobalt and manganese elements on catalyst surface were recorded in an ESCALAB250 spectrometer using $\text{Al K}\alpha$ radia-

tion with pass energy of 20 eV. The charging effect was corrected by referencing C 1s peak centered at 284.6 eV.

2 Results and discussion

2.1 Catalytic activity of Mn-Co-Al spinel oxides with different compositions

The XRD patterns of $Mn_xCo_{2.5-x}Al_{0.5}O_4$ oxides with different compositions are shown in Figure 1, several diffraction peaks attributed to the crystallographic planes of (311), (220), (511), (440) in spinel-structured materials are observed. It can be found that the diffraction angles move to lower values with the increase of Mn contents due to the radius difference between cobalt and manganese ions.

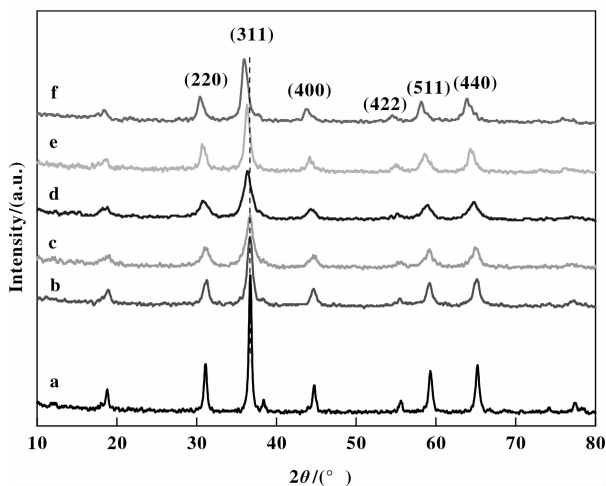


Fig. 1 XRD patterns of Mn-Co-Al spinel oxides with different compositions

- a. $Co_{2.5}Al_{0.5}O_4$; b. $Mn_{0.2}Co_{2.3}Al_{0.5}O_4$;
c. $Mn_{0.4}Co_{2.1}Al_{0.5}O_4$; d. $Mn_{0.6}Co_{1.9}Al_{0.5}O_4$;
e. $Mn_{0.8}Co_{1.7}Al_{0.5}O_4$; f. $MnCo_{1.5}Al_{0.5}O_4$

Figure 2 presents the N_2O conversions over different Mn-Co-Al oxides. It is shown that the $Mn_{0.2}Co_{2.3}Al_{0.5}O_4$ reveals a maximum activity, and other $Mn_xCo_{2.5-x}Al_{0.5}O_4$ catalysts with x values higher than 0.6 are inferior to $Co_{2.5}Al_{0.5}O_4$. As listed in Table 1, the BET surface area of Mn-Co-Al oxides especially $Mn_{0.2}Co_{2.3}Al_{0.5}O_4$ of $77.7 \text{ m}^2 \cdot \text{g}^{-1}$ is larger than $Co_{2.5}Al_{0.5}O_4$, responding to the higher activity of $Mn_{0.2}Co_{2.3}Al_{0.5}O_4$ than $Co_{2.5}Al_{0.5}O_4$.

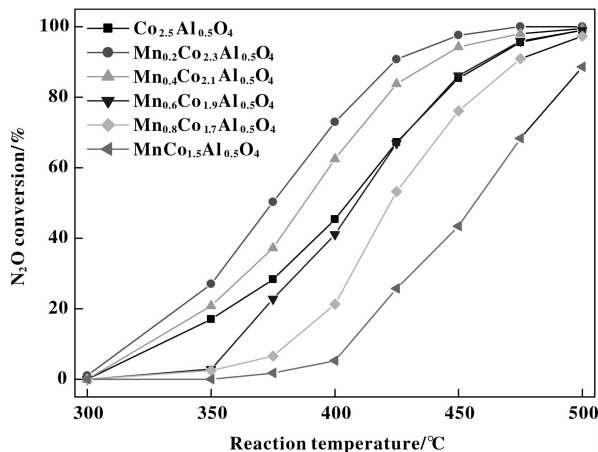


Fig. 2 N_2O conversions over Mn-Co-Al spinel oxides with different compositions

Table 1 BET surface area of Mn-Co-Al spinel oxides with different compositions

Catalysts	BET surface area / ($\text{m}^2 \cdot \text{g}^{-1}$)
$Co_{2.5}Al_{0.5}O_4$	41.2
$Mn_{0.2}Co_{2.3}Al_{0.5}O_4$	77.7
$Mn_{0.4}Co_{2.1}Al_{0.5}O_4$	71.4
$Mn_{0.6}Co_{1.9}Al_{0.5}O_4$	60.8
$Mn_{0.8}Co_{1.7}Al_{0.5}O_4$	58.4
$MnCo_{1.5}Al_{0.5}O_4$	58.8

Figure 3 (A) shows the H_2 -TPR profiles of catalysts. Considering the catalytic components reducibility higher than 500 °C of the maximum reaction temperature in our study can not likely contribute to the oxygen mobility and catalytic reaction, the hydrogen consumed below 500 °C is separated and shown in Figure 3 (A). We can find a wide peak at the region of 310 ~ 480 °C attributed to the reduction of $Co^{3+} \rightarrow Co^{2+}$ in $Co_{2.5}Al_{0.5}O_4$ and plus $Mn_3O_4 \rightarrow MnO$ in $Mn_{0.2}Co_{2.3}Al_{0.5}O_4$. With high content of Mn, the other peak centered at 273 °C is found in $Mn_{0.4}Co_{2.1}Al_{0.5}O_4$ and $MnCo_{1.5}Al_{0.5}O_4$ catalysts and ascribed to the reduction of Mn_2O_3 (or MnO_2) $\rightarrow Mn_3O_4$, these free manganese oxides from spinel-structure seem to produce a detrimental effect on catalytic activity^[18].

O_2 -TPD profiles of $Mn_xCo_{2.5-x}Al_{0.5}O_4$ catalysts are

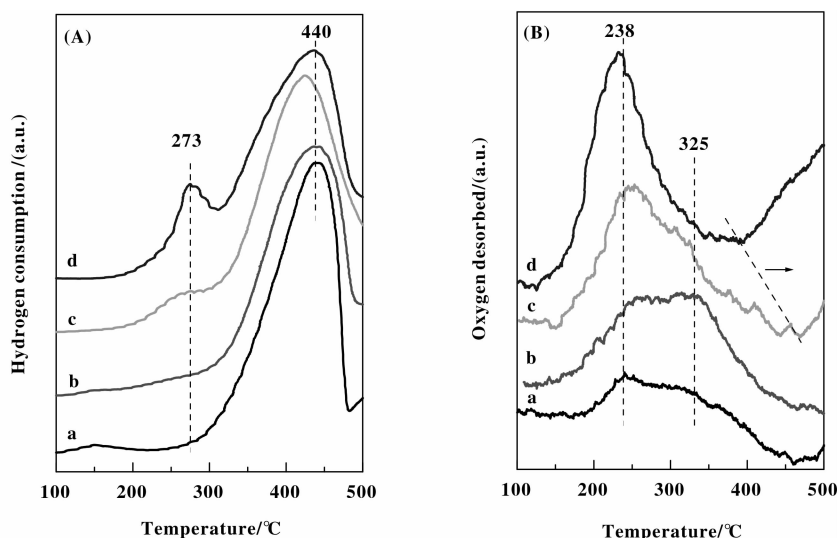


Fig. 3 (A) H_2 -TPR and (B) O_2 -TPD profiles of Mn-Co-Al spinel oxides with different compositions

a. $\text{Co}_{2.5}\text{Al}_{0.5}\text{O}_4$; b. $\text{Mn}_{0.2}\text{Co}_{2.3}\text{Al}_{0.5}\text{O}_4$; c. $\text{Mn}_{0.4}\text{Co}_{2.1}\text{Al}_{0.5}\text{O}_4$; d. $\text{MnCo}_{1.5}\text{Al}_{0.5}\text{O}_4$

shown in Figure 3 (B). The peak centered at 238 °C on all catalysts can be ascribed to the weakly adsorbed oxygen species, and the other peak around 325 °C only on $\text{Co}_{2.5}\text{Al}_{0.5}\text{O}_4$ and $\text{Mn}_{0.2}\text{Co}_{2.3}\text{Al}_{0.5}\text{O}_4$ catalysts surface is assigned to strongly adsorbed oxygen^[22]. Obviously, a high-temperature peak at the beginning of ca. 400 °C attributed to lattice oxygen appears on $\text{Mn}_{0.4}\text{Co}_{2.1}\text{Al}_{0.5}\text{O}_4$ and $\text{MnCo}_{1.5}\text{Al}_{0.5}\text{O}_4$ catalysts. It is thought that the active sites on catalysts surface for strong adsorption of oxygen ($\text{O}=\text{O}$) are effective for N_2O ($\text{N}=\text{O}$) activation in N_2O decomposition. The $\text{Mn}_{0.2}\text{Co}_{2.3}\text{Al}_{0.5}\text{O}_4$ can strongly adsorb more amounts of oxygen, and therefore reveal higher activity than other catalysts for N_2O decomposition.

2.2 Catalytic activity of $\text{Mn}_{0.2}\text{Co}_{2.3}\text{Al}_{0.5}\text{O}_4$ composite oxides prepared by mother liquids with different pH values

The XRD patterns of $\text{Mn}_{0.2}\text{Co}_{2.3}\text{Al}_{0.5}\text{O}_4$ prepared by mother liquids with different pH values are shown in Figure 4. We can find the diffraction peaks ascribed to crystallographic planes of (220), (311), (400), (422), and (511) in spinels, and the difference of mother liquid pH values has not changed the catalysts structure. As shown in Figure 5, these catalysts are dispersive nano-particles.

Figure 6 gives the N_2O conversions over different $\text{Mn}_{0.2}\text{Co}_{2.3}\text{Al}_{0.5}\text{O}_4$ catalysts, and their activity follows

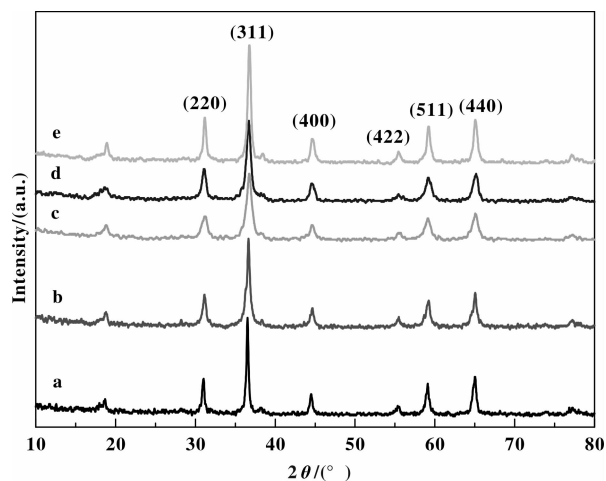


Fig. 4 XRD patterns of $\text{Mn}_{0.2}\text{Co}_{2.3}\text{Al}_{0.5}\text{O}_4$ prepared by mother liquids with different pH values

a. pH=0.5; b. pH=1; c. pH=2; d. pH=3; e. pH=4

the order of pH = 2 > pH = 1 > pH = 3 > pH = 4 > pH = 0.5. Of these catalysts, the $\text{Mn}_{0.2}\text{Co}_{2.3}\text{Al}_{0.5}\text{O}_4$ (pH = 2) and $\text{Mn}_{0.2}\text{Co}_{2.3}\text{Al}_{0.5}\text{O}_4$ (pH = 1) reveal higher activity than others. As listed in Table 2, when the pH of mother liquids is adjusted to higher values, the as-prepared catalysts become smaller with increase in surface area. It is notable that the $\text{Mn}_{0.2}\text{Co}_{2.3}\text{Al}_{0.5}\text{O}_4$ (pH = 2) particle is as small as 12.2 nm and its surface area as high as $77.7 \text{ m}^2 \cdot \text{g}^{-1}$. These characteristic features agree well with the catalytic activity, e. g. small crystallites and large surface area of catalysts respond to high activity.

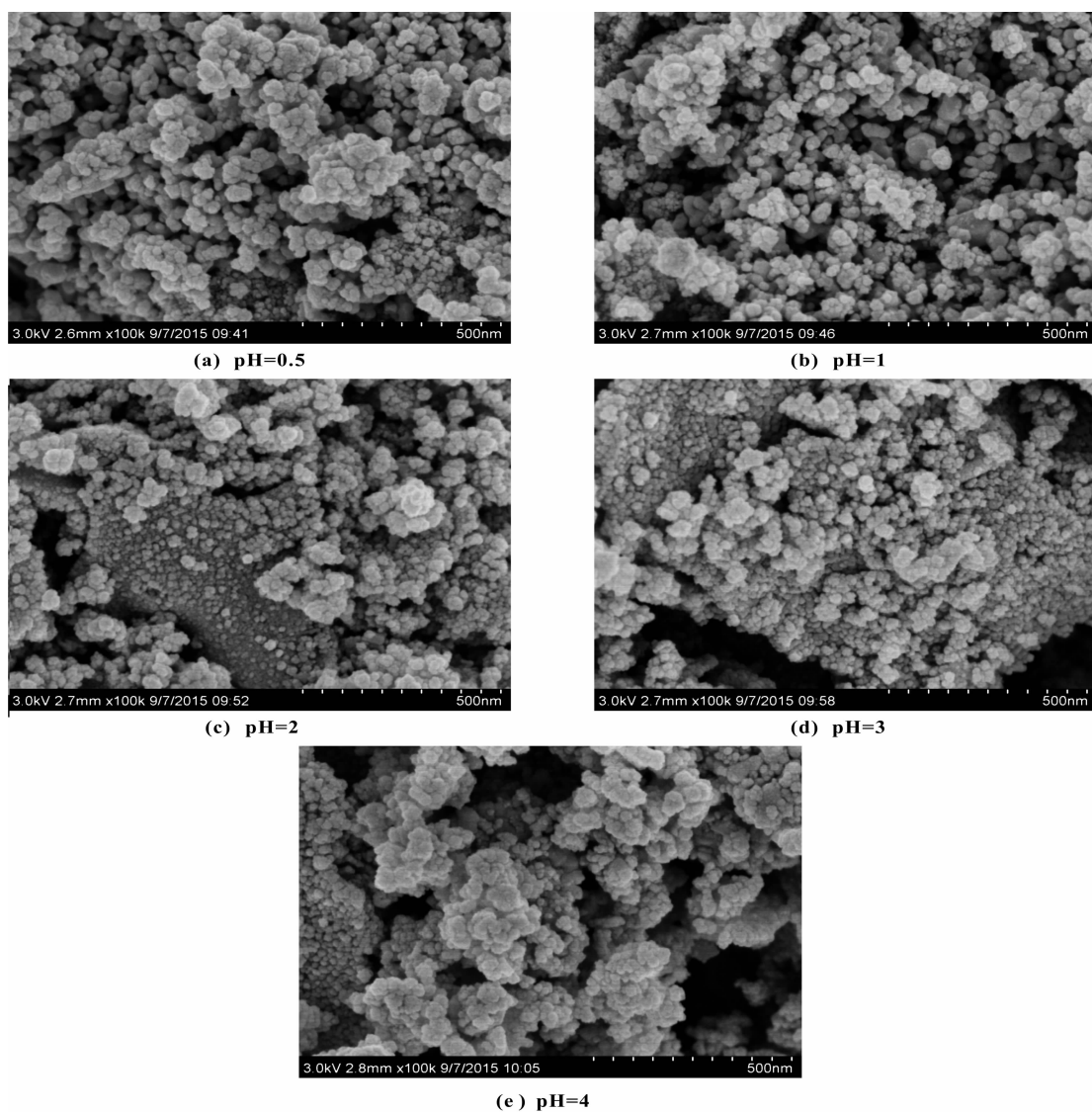


Fig. 5 SEM images of $Mn_{0.2}Co_{2.3}Al_{0.5}O_4$ prepared by mother liquids with different pH values

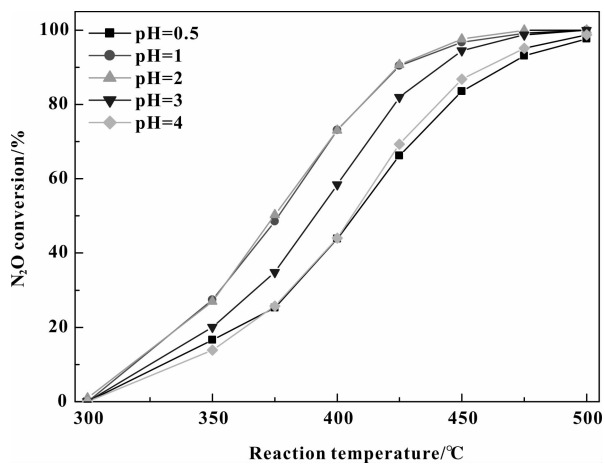


Fig. 6 N_2O conversions over $Mn_{0.2}Co_{2.3}Al_{0.5}O_4$ prepared with different pH values of mother liquid

Table 2 Crystallite size and BET surface area of $Mn_{0.2}Co_{2.3}Al_{0.5}O_4$ prepared by mother liquids with different pH values

Catalysts	Crystallite size	BET surface area
	/nm ^a	/ $(m^2 \cdot g^{-1})$
$Mn_{0.2}Co_{2.3}Al_{0.5}O_4$ (pH=0.5)	72.9	32.8
$Mn_{0.2}Co_{2.3}Al_{0.5}O_4$ (pH=1)	41.1	36.4
$Mn_{0.2}Co_{2.3}Al_{0.5}O_4$ (pH=2)	12.2	77.7
$Mn_{0.2}Co_{2.3}Al_{0.5}O_4$ (pH=3)	15.6	54.9
$Mn_{0.2}Co_{2.3}Al_{0.5}O_4$ (pH=4)	19.9	43.0

a. Calculated by Scherrer equation on the basis of (311) crystallographic plane data in XRD patterns.

2.3 Catalytic activity of K-modified $\text{Mn}_{0.2}\text{Co}_{2.3}\text{Al}_{0.5}\text{O}_4$ catalysts

In order to further improve the catalytic activity, the optimized catalyst of $\text{Mn}_{0.2}\text{Co}_{2.3}\text{Al}_{0.5}\text{O}_4$ (pH=2) is modified by K_2CO_3 . The XRD characterization result indicates that all of the K-doped catalysts are spinel-structure without free K-related phases. Figure 7 shows the N_2O conversion on K/ $\text{Mn}_{0.2}\text{Co}_{2.3}\text{Al}_{0.5}\text{O}_4$ (pH = 2)

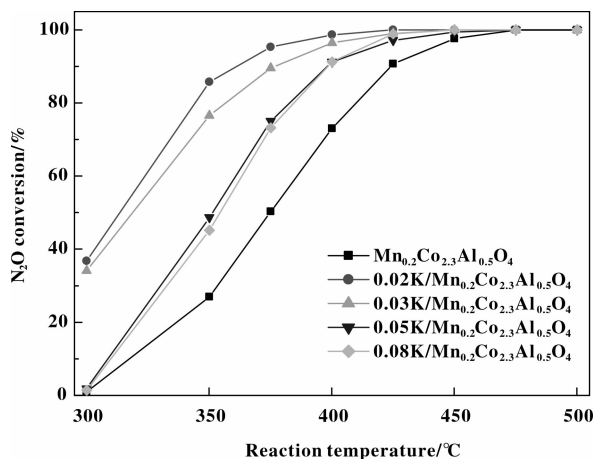


Fig. 7 N_2O conversions of K/ $\text{Mn}_{0.2}\text{Co}_{2.3}\text{Al}_{0.5}\text{O}_4$ with different potassium loadings

catalysts, K-modified catalysts present higher activity in contrast to bare catalyst. Especially, N_2O can be completely destructed at 425 °C over 0.02 K/ $\text{Mn}_{0.2}\text{Co}_{2.3}\text{Al}_{0.5}\text{O}_4$, which exhibits higher activity than others. As listed in Table 3, the addition of K leads to a decrease in surface area and an increase in crystallite unfavorable to catalysts activity. What is the more

Table 3 Crystallite size and BET surface area of K/ $\text{Mn}_{0.2}\text{Co}_{2.3}\text{Al}_{0.5}\text{O}_4$ with different potassium loadings

Catalysts	Crystallite size BET surface area	
	/nm ^a	/(m ² · g ⁻¹)
$\text{Mn}_{0.2}\text{Co}_{2.3}\text{Al}_{0.5}\text{O}_4$	12.2	77.7
0.02 K/ $\text{Mn}_{0.2}\text{Co}_{2.3}\text{Al}_{0.5}\text{O}_4$	16.2	67.8
0.03 K/ $\text{Mn}_{0.2}\text{Co}_{2.3}\text{Al}_{0.5}\text{O}_4$	17.3	69.4
0.05 K/ $\text{Mn}_{0.2}\text{Co}_{2.3}\text{Al}_{0.5}\text{O}_4$	21.3	66.2
0.08 K/ $\text{Mn}_{0.2}\text{Co}_{2.3}\text{Al}_{0.5}\text{O}_4$	15.1	67.2

a. Calculated by Scherrer equation on the basis of (311) crystallographic plane data in XRD patterns.

important influencing factor than surface area or crystallite size on catalysts activity?

Figure 8 and 9 shows the XPS spectra of Co 2p and Mn 2p on K/ $\text{Mn}_{0.2}\text{Co}_{2.3}\text{Al}_{0.5}\text{O}_4$ catalysts. Table 4

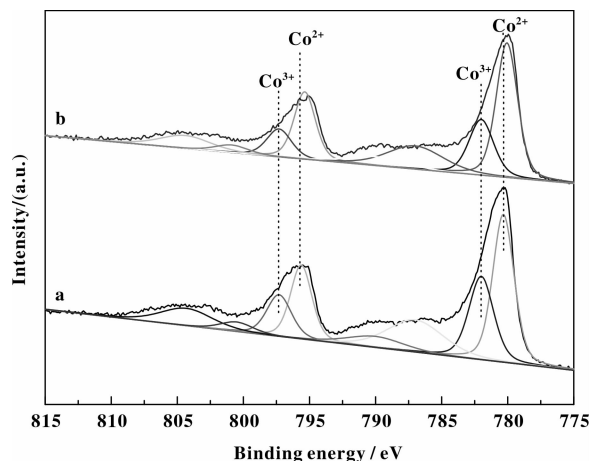


Fig. 8 XPS spectra of Co 2p in K/ $\text{Mn}_{0.2}\text{Co}_{2.3}\text{Al}_{0.5}\text{O}_4$ catalyst
a. $\text{Mn}_{0.2}\text{Co}_{2.3}\text{Al}_{0.5}\text{O}_4$; b. 0.02 K/ $\text{Mn}_{0.2}\text{Co}_{2.3}\text{Al}_{0.5}\text{O}_4$

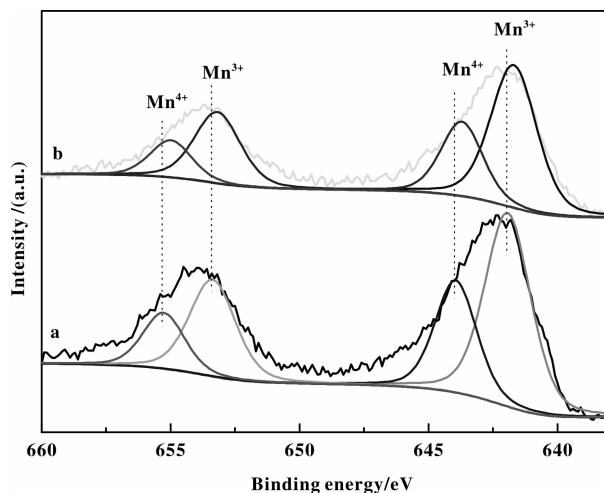


Fig. 9 XPS spectra of Mn 2p in K/ $\text{Mn}_{0.2}\text{Co}_{2.3}\text{Al}_{0.5}\text{O}_4$ catalyst
a. $\text{Mn}_{0.2}\text{Co}_{2.3}\text{Al}_{0.5}\text{O}_4$; b. 0.02 K/ $\text{Mn}_{0.2}\text{Co}_{2.3}\text{Al}_{0.5}\text{O}_4$

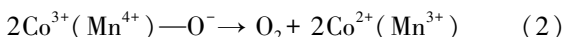
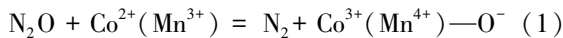
lists the fitting data of Co $2p_{3/2}$ and Mn $2p_{3/2}$ peaks. In the case of $\text{Mn}_{0.2}\text{Co}_{2.3}\text{Al}_{0.5}\text{O}_4$, the Co $2p_{3/2}$ peaks centered at 780.3 eV and 782.0 eV can be assigned to Co^{2+} and Co^{3+} , the peaks of Mn $2p_{3/2}$ centered at 641.7 eV and 643.8 eV are assigned to Mn^{3+} and Mn^{4+} . In comparison with un-modified catalyst, the binding energies of Mn $2p_{3/2}$ and Co $2p_{3/2}$ on 0.02 K/ $\text{Mn}_{0.2}\text{Co}_{2.3}\text{Al}_{0.5}\text{O}_4$ (pH=2) shift to lower values of 0.2 eV. The reduction in binding energies indicates that

Table 4 XPS data of $K/Mn_{0.2}Co_{2.3}Al_{0.5}O_4$ catalysts

Catalysts	Binding energies of Co $2p_{3/2}/eV$		Co^{2+}/Co^{3+}	Binding energies of Mn $2p_{3/2}/eV$		Mn^{3+}/Mn^{4+}
	Co^{2+}	Co^{3+}		Mn^{3+}	Mn^{4+}	
$Mn_{0.2}Co_{2.3}Al_{0.5}O_4$	780.3	782.0	1.85	641.9	643.9	1.91
$0.02K/Mn_{0.2}Co_{2.3}Al_{0.5}O_4$	780.1	782.0	2.23	641.7	643.7	2.12

the electron donation from K causes a change in the electronic state of Co and Mn, which results in the weakness of Mn-O and Co-O bonds, and easy removal of oxygen species, thus the improved catalytic activity.

As listed in Table 4, we can find the molar ratios of Co^{2+}/Co^{3+} and Mn^{3+}/Mn^{4+} on K-modified catalysts are higher than un-modified catalyst. As stated in Equations (1-2), the oxidation-reduction cycles between Mn^{3+} and $Mn^{4+}-O^-$, Co^{2+} and $Co^{3+}-O^-$ take place in N_2O decomposition, it can be speculated that more Co^{2+} and Mn^{3+} ions in K-modified catalysts produce more active sites and present higher activity.



2.4 Catalytic activity and stability of $K/Mn_{0.2}Co_{2.3}Al_{0.5}O_4$ in oxygen and steam

In this part, the catalytic activity and stability of $0.02 K/Mn_{0.2}Co_{2.3}Al_{0.5}O_4$ catalyst under various atmospheres have been tested. Figure 10 shows the initial activity of $Mn_{0.2}Co_{2.3}Al_{0.5}O_4$ and K-modified catalysts, it is found that the catalyst activity decreases in the presence of steam as the water molecules

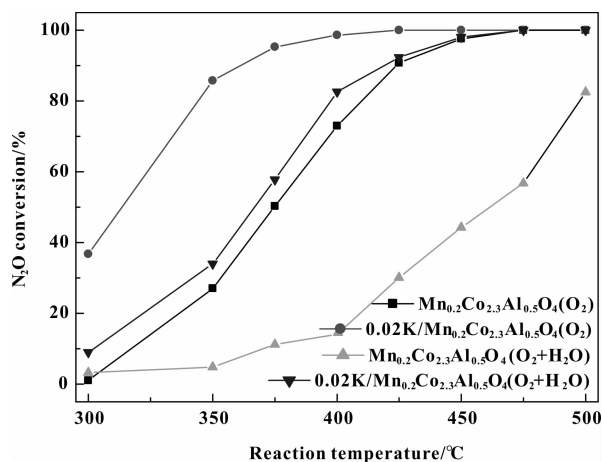


Fig. 10 N_2O conversions on $K/Mn_{0.2}Co_{2.3}Al_{0.5}O_4$ in the presence of oxygen and steam

occupy the active sites on catalysts surface and prevent the N_2O adsorption.

As shown in Figure 11, both bare and K-doped catalysts are stable in N_2O decomposition. It is different that after continuous running for 50 h at 400 °C in

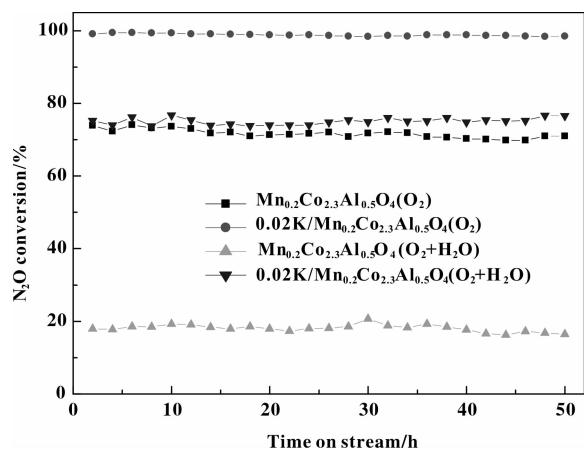


Fig. 11 Catalytic stability of $K/Mn_{0.2}Co_{2.3}Al_{0.5}O_4$ catalyst for N_2O decomposition at 400 °C

oxygen-alone and oxygen-steam together, N_2O conversions over $0.02 K/Mn_{0.2}Co_{2.3}Al_{0.5}O_4$ could keep 98.5% and 76.5% respectively, while that on un-doped catalyst is only 71.0% and 16.4%, indicating K-doped catalyst exhibits higher activity and better resistance towards water than un-doped catalyst.

3 Conclusions

A series of $Mn_xCo_{2.5-x}Al_{0.5}O_4$ ternary spinel oxides were prepared by sol-gel method and further modified by K_2CO_3 . The effect of composite oxide compositions, pH values of mother liquid, and potassium loadings on catalytic activity for N_2O decomposition was investigated. The results show that K-modified catalysts exhibit higher catalytic activity and better reducibility than bare catalyst due to the weaker metal-oxygen bonds on

catalyst surface. Among these catalysts, the $\text{K}/\text{Mn}_{0.2}\text{Co}_{2.3}\text{Al}_{0.5}\text{O}_4$ prepared with mother liquid of $\text{pH}=2$ and $\text{K}/(\text{Mn}+\text{Co})$ molar ratio of 0.02 is the most active one, over which 98.5% and 76.5% conversions of N_2O could be kept at 400 °C after 50 h in oxygen-only and oxygen-stream together, respectively.

References:

- [1] Kapteijn F, Rodriguez-Mirasol J, Moulijn J A. Heterogeneous catalytic decomposition of nitrous oxide [J]. *Appl Catal B: Environ*, 1996, **9**(1/4): 25–64.
- [2] a. Beyer H, Emmerich J, Chatziapostolou K, *et al.* Decomposition of nitrous oxide by rhodium catalysts: Effect of rhodium particle size and metal oxide support [J]. *Appl Catal A: Gen*, 2011, **391**(1/2): 411–416.
b. Zong Yue(宗 玥), Li Meng-li(李孟丽), Yang Xiaolong(杨晓龙), *et al.* Ru supported on foamed aluminum applied in the low-temperature catalytic decomposition of N_2O (泡沫铝负载钉基催化剂应用于 N_2O 的低温催化分解研究) [J]. *J Mol Catal (China)* (分子催化), 2014, **28**(4): 336–343.
- [3] Dou Z, Feng M, Xu X F. Catalytic decomposition of N_2O over $\text{Au}/\text{Co}_3\text{O}_4$ and $\text{Au}/\text{ZnCo}_2\text{O}_4$ catalysts [J]. *J Fuel Chem Tech*, 2013, **41**(10): 1234–1240.
- [4] Xu X L, Xu X F, Zhang G T, *et al.* Preparation of Co-Al mixed oxide-supported gold catalysts and their catalytic activity for N_2O decomposition [J]. *J Fuel Chem Tech*, 2009, **37**(5): 595–600.
- [5] Xie P F, Luo Y J, Ma Z, *et al.* Catalytic decomposition of N_2O over Fe-ZSM-11 catalysts prepared by different methods: Nature of active Fe species [J]. *J Catal*, 2015, **330**: 311–322.
- [6] Boroń P, Chmielarz L, Gurgul J, *et al.* The influence of the preparation procedures on the catalytic activity of Fe-BEA zeolites in SCR of NO with ammonia and N_2O decomposition [J]. *Catal Today*, 2014, **235**: 210–225.
- [7] Cürdaneli P E, Özkar S. Ruthenium (III) ion-exchanged zeolite Y as highly active and reusable catalyst in decomposition of nitrous oxide to sole nitrogen and oxygen [J]. *Micro Mes Mat*, 2014, **196**: 51–58.
- [8] Karásková K, Obalová L, Jirátková K, *et al.* Effect of promoters in Co-Mn-Al mixed oxide catalyst on N_2O decomposition [J]. *Chem Eng J*, 2010, **160**(2): 480–487.
- [9] Wang Jian (王建), Zhang Hai-jie (张海杰), Xu Xiufeng (徐秀峰). Catalytic decomposition of N_2O over $\text{Cu}_x\text{Fe}_{1-x}\text{Fe}_2\text{O}_4$ and $\text{Ni}_x\text{Fe}_{1-x}\text{Fe}_2\text{O}_4$ spinel oxides (N_2O 在 $\text{Cu}_x\text{Fe}_{1-x}\text{Fe}_2\text{O}_4$ 和 $\text{Ni}_x\text{Fe}_{1-x}\text{Fe}_2\text{O}_4$ 复合氧化物催化剂上的分解反应) [J]. *J Mol Catal (China)* (分子催化), 2015, **29**(1): 75–80.
- [10] Amrousse R, Katsumi T. Substituted ferrite $\text{M}_x\text{Fe}_{1-x}\text{Fe}_2\text{O}_4$ ($\text{M}=\text{Mn}, \text{Zn}$) catalysts for N_2O catalytic decomposition processes [J]. *Catal Commun*, 2012, **26**: 194–198.
- [11] Xue L, He H, Liu C, *et al.* Promotion effects and mechanism of alkali metals and alkaline earth metals on cobalt-cerium composite oxide catalysts for N_2O decomposition [J]. *Environ Sci Technol*, 2009, **43**(3): 890–895.
- [12] Abu-Zied B M, Soliman S A, Abdellah S E. Pure and Ni-substituted Co_3O_4 spinel catalysts for direct N_2O decomposition [J]. *Chin J Catal*, 2014, **35**(7): 1105–1112.
- [13] Yan L, Ren T, Wang X, *et al.* Catalytic decomposition of N_2O over $\text{M}_x\text{Co}_{1-x}\text{Co}_2\text{O}_4$ ($\text{M}=\text{Ni}, \text{Mg}$) spinel oxides [J]. *Appl Catal B: Environ*, 2003, **45**(2): 85–90.
- [14] Obalová L, Karásková K, Wach A, *et al.* Alkali metals as promoters in Co-Mn-Al mixed oxide for N_2O decomposition [J]. *Appl Catal A: Gen*, 2013, **462/463**: 227–235.
- [15] Kondratenko E V, Kondratenko V A, Santiago M, *et al.* Mechanism and micro-kinetics of direct N_2O decomposition over $\text{BaFeAl}_{11}\text{O}_{19}$ hexaaluminate and comparison with Fe-MFI zeolites [J]. *Appl Catal B: Environ*, 2010, **99**(1/2): 66–73.
- [16] Wang Jian (王建), Wu Cang-cang(吴藏藏), Zheng Li (郑丽), *et al.* Catalytic decomposition of N_2O over $\text{Ce}_x\text{Co}_{2-x}\text{AlO}_4$ composite oxides prepared by sol-gel method (溶胶凝胶法制备 $\text{Ce}_x\text{Co}_{2-x}\text{AlO}_4$ 复合氧化物及其催化分解 N_2O) [J]. *J Mol Catal (China)* (分子催化), 2015, **29**(6): 553–562.
- [17] Karásková K, Obalová L, Kovanda F. N_2O catalytic decomposition and temperature programmed desorption tests on alkali metals promoted Co-Mn-Al mixed oxide [J]. *Catal Today*, 2011, **176**(1): 208–211.
- [18] Wang Jian (王建), Dou Zhe (窦喆), Pan Yan-fei (潘燕飞), *et al.* Catalytic decomposition of N_2O over $\text{Mn}_x\text{Co}_{3-x}\text{O}_4$ mixed oxides and modified catalysts ($\text{Mn}_x\text{Co}_{3-x}\text{O}_4$ 复合氧化物及改性催化剂催化分解 N_2O) [J]. *J Mol Catal (China)* (分子催化), 2015, **29**(3): 246–255.
- [19] Ohnishi C, Asano K, Iwamoto S, *et al.* Alkali-doped Co_3O_4 catalysts for direct decomposition of N_2O in the presence of oxygen [J]. *Catal Today*, 2007, **120**(2):

- 145-150.
- [20] Wu H P, Qian Z Y, Xu X L, *et al.* N_2O decomposition over K-promoted NiAl mixed oxides derived from hydrocalcite-like compounds [J]. *J Fuel Chem Tech*, 2011, **39**(2): 115-121.
- [21] Dou Z, Zhang H J, Pan Y F, *et al.* Catalytic decomposition of N_2O over potassium-modified Cu-Co spinel oxides [J]. *J Fuel Chem Tech*, 2014, **42**(2): 238-245.
- [22] Franken T, Palkovits R. Investigation of potassium doped mixed spinels $Cu_xCo_{3-x}O_4$ as catalysts for an efficient N_2O decomposition in real reaction conditions [J]. *Appl Catal B: Environ*, 2015, **176/177**: 298-305.
- [23] Zhang H J, Wang J, Xu X F. Catalytic decomposition of N_2O over $Ni_xCo_{1-x}CoAlO_4$ spinel oxides prepared by sol-gel method[J]. *J Fuel Chem Tech*, 2015, **43**(1): 81-87.
- [24] Wu Cang-cang (吴藏藏), Zhang Hai-jie (张海杰), Wang Jian (王建), *et al.* The preparation parameters screening of Co-Al spinel oxides for N_2O catalytic decomposition (N_2O 分解催化剂 Co-Al 尖晶石型复合氧化物制备参数的优化) [J]. *J Mol Catal(China)* (分子催化), 2016, **30**(1): 62-71.

$Mn_xCo_{2.5-x}Al_{0.5}O_4$ 尖晶石型三元复合氧化物 催化分解 N_2O

吴藏藏, 张海杰, 王建, 郑丽, 徐秀峰*

(烟台大学 应用催化研究所, 山东 烟台 264005)

摘要: 用溶胶凝胶法制备了一组 $Mn_xCo_{2.5-x}Al_{0.5}O_4$ 尖晶石型三元复合氧化物, 用于有氧气氛下的 N_2O 催化分解反应. 用 N_2 物理吸附、X 射线衍射 (XRD)、扫描电镜 (SEM)、 H_2 程序升温还原 (H_2 -TPR)、 O_2 程序升温脱附 (O_2 -TPD)、X 射线光电子能谱 (XPS) 等技术对催化剂进行了结构表征, 考察了催化剂组成、母液 pH、K 负载量等制备参数对其催化活性的影响. 结果表明: K 的加入弱化了催化剂表面的金属-氧化学键, 有利于表面氧物种的脱除, 改性催化剂有较高的催化活性和抗水性, 其中母液 pH=2、K/(Mn+Co) 比为 0.02 的 $K/Mn_{0.2}Co_{2.3}Al_{0.5}O_4$ 催化剂活性较高, 该催化剂在有氧、有氧有水气氛 400 °C 连续反应 50 h, N_2O 转化率分别达 98.5% 和 76.5%.

关键词: N_2O 催化分解; 尖晶石型三元复合氧化物; $Mn_xCo_{2.5-x}Al_{0.5}O_4$; 溶胶凝胶法; K 改性催化剂